

Supplementary Movie 1. Baseline TE α CD4⁺ T-cell velocity and motility in brachial lymph nodes. B6 eGFP-TE α CD4⁺ T-cells (green) and CMTMR-labeled OT-I CD8⁺ T-cells (red) were transferred in to lethally irradiated CB6.F1-CD11c-YFP mice. Brachial lymph nodes were imaged for 30 minutes with multi-photon microscopy 2 days after TE α and OT-I transfer. To better visualize T-cells, YFP positive antigen presenting cells are not shown.

Supplementary Movie 2. DMSO treated Treg increase TE α CD4⁺ T-cell motility and velocity compared to mice that did not receive Treg. B6 eGFP-TE α CD4⁺ T-cells (green), CMTMR-labeled OT-I CD8⁺ T-cells (red), and unstained WT DMSO pre-treated Treg were transferred in to lethally irradiated CB6.F1-CD11c-YFP mice. Brachial lymph nodes were imaged for 30 minutes with multi-photon microscopy 2 days after TE α and OT-I transfer. To better visualize T-cells, YFP positive antigen presenting cells are not shown.

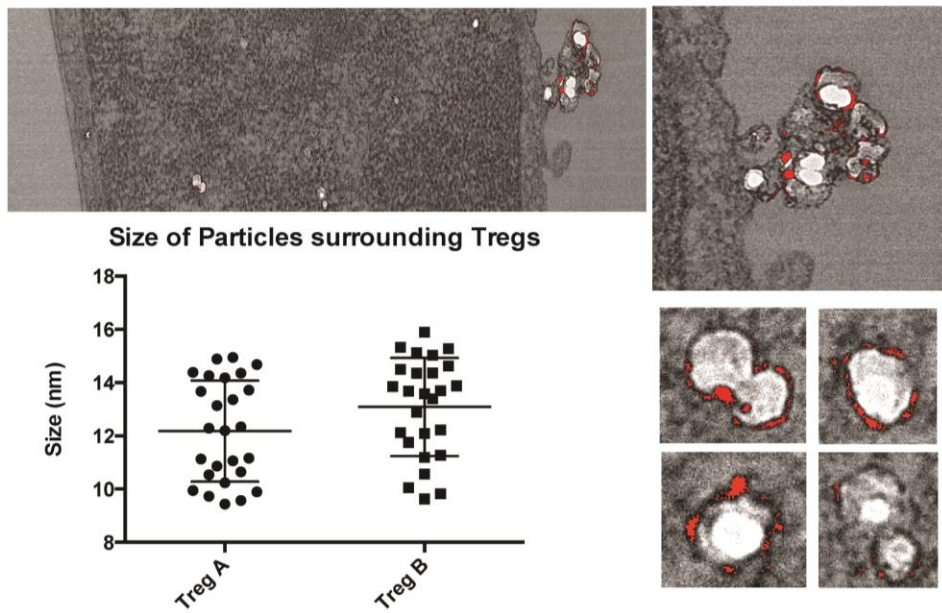
Supplementary Movie 3. AEB071 treated Treg increase TE α CD4⁺ T-cell motility and velocity compared to DMSO treated Treg (vehicle control). B6 eGFP-TE α CD4⁺ T-cells (green), CMTMR-labeled OT-I CD8⁺ T-cells (red), and unstained WT AEB071 pre-treated Treg were transferred in to lethally irradiated CB6.F1-CD11c-YFP mice. Brachial lymph nodes were imaged for 30 minutes with multi-photon microscopy 2 days after TE α and OT-I transfer. To better visualize T-cells, YFP positive antigen presenting cells are not shown.

Supplementary Movie 4. Baseline TE α CD4⁺ T-cell velocity and motility in mesenteric lymph nodes. B6 eGFP-TE α CD4⁺ T-cells (green) and CMTMR-labeled OT-I CD8⁺ T-cells (red) were transferred in to lethally irradiated CB6.F1-CD11c-YFP mice. Mesenteric lymph nodes were imaged for 30 minutes with multi-photon microscopy 2 days after TE α and OT-I transfer. To better visualize T-cells, YFP positive antigen presenting cells are not shown.

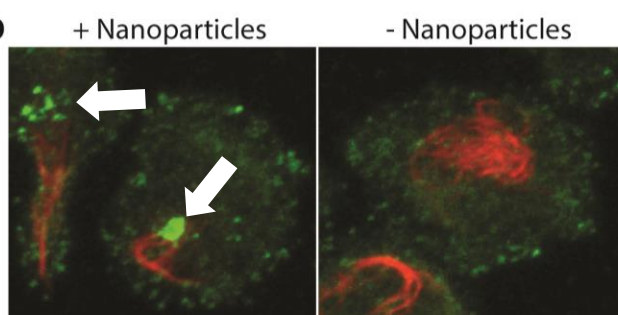
Supplementary Movie 5. DMSO treated Treg increase TE α CD4⁺ T-cell motility and velocity in mesenteric lymph nodes compared to mice that did not receive Treg. B6 eGFP-TE α CD4⁺ T-cells (green), CMTMR-labeled OT-I CD8⁺ T-cells (red), and unstained WT DMSO pre-treated Treg were transferred in to lethally irradiated CB6.F1-CD11c-YFP mice. Mesenteric lymph nodes were imaged for 30 minutes with multi-photon microscopy 2 days after TE α and OT-I transfer. To better visualize T-cells, YFP positive antigen presenting cells are not shown.

Supplementary Movie 6. AEB071 treated Treg increase TE α CD4⁺ T-cell motility and velocity in mesenteric lymph nodes compared to DMSO treated Treg (vehicle control). B6 eGFP-TE α CD4⁺ T-cells (green), CMTMR-labeled OT-I CD8⁺ T-cells (red), and unstained WT AEB071 pre-treated Treg were transferred in to lethally irradiated CB6.F1-CD11c-YFP mice. Mesenteric lymph nodes were imaged for 30 minutes with multi-photon microscopy 2 days after TE α and OT-I transfer. To better visualize T-cells, YFP positive antigen presenting cells are not shown.

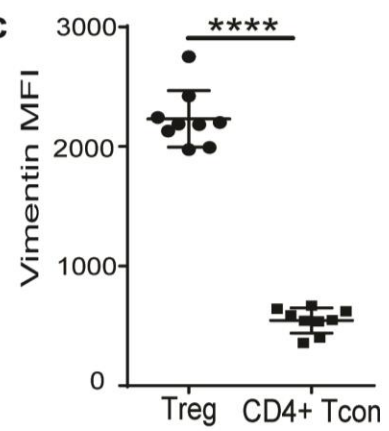
a



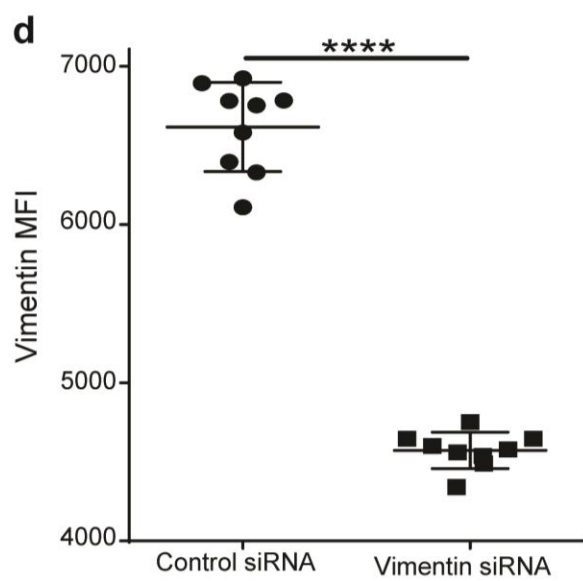
b



c



d

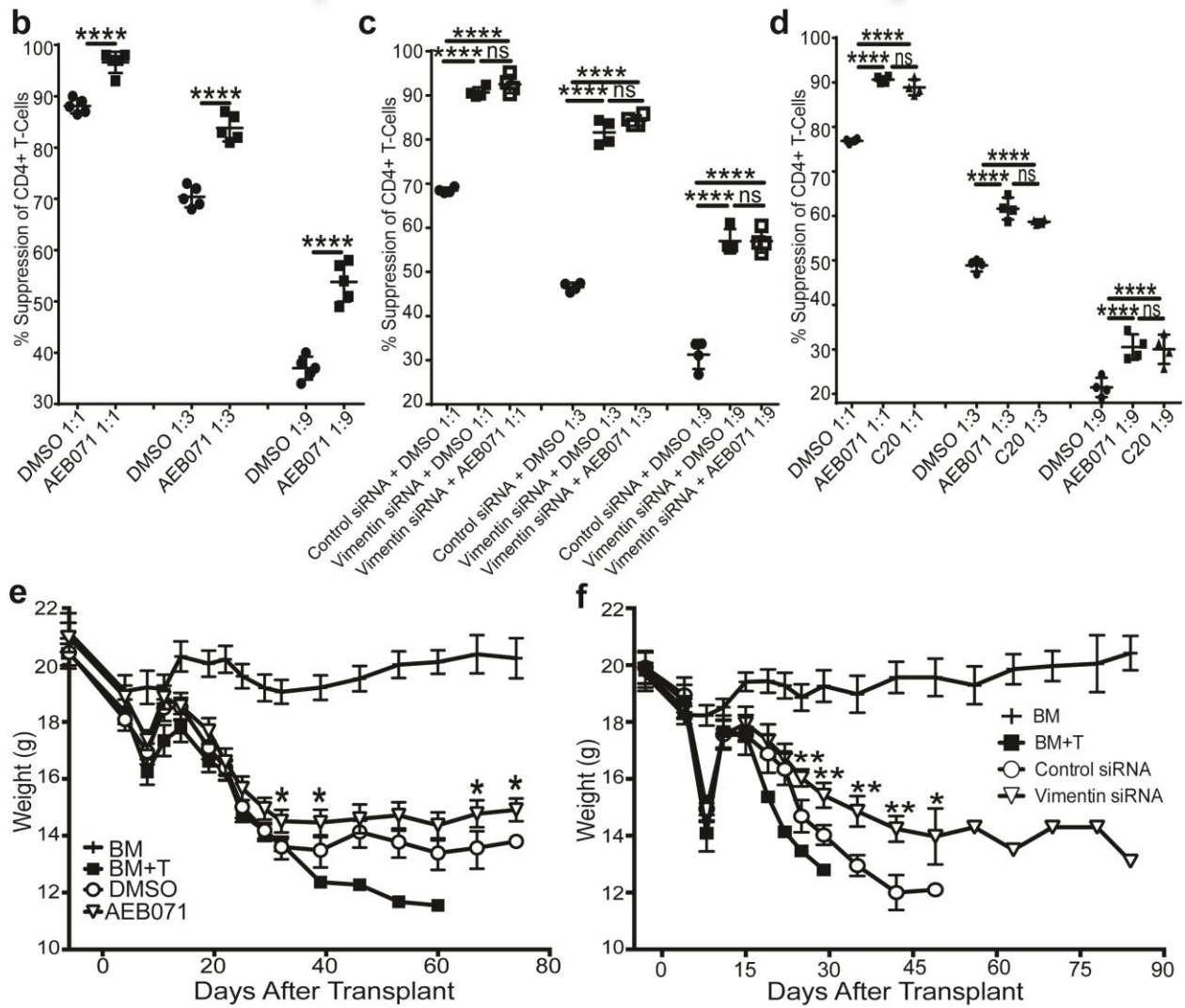
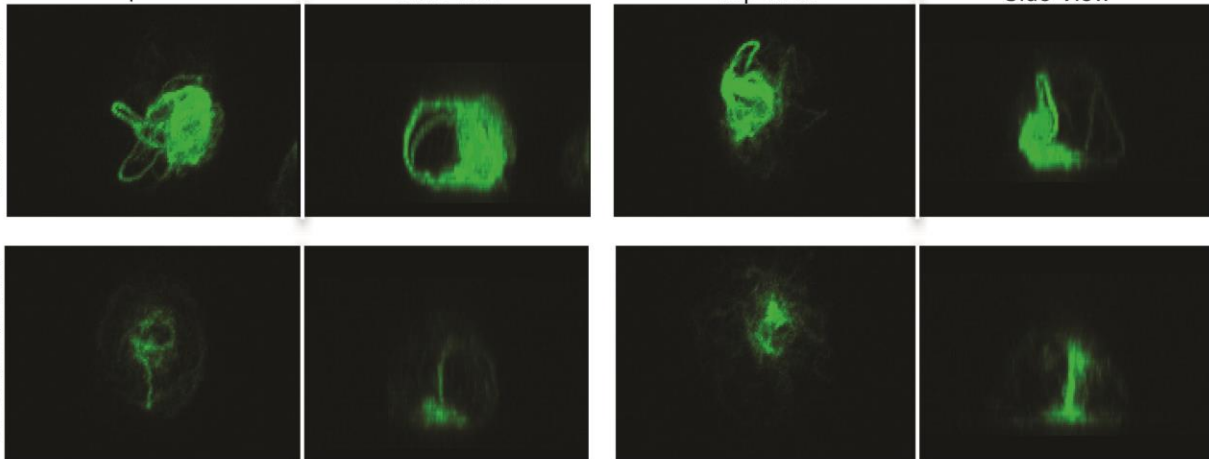


Supplementary Figure 1. PKC- θ and vimentin complex together in activated Treg. (a) Electron microscopy of nanoparticle treated Treg showing nanoparticle accumulation in Treg, with quantification of the size of nanoparticles, corresponding to the expected size for the iron core (12-14nm). **(b)** Confocal microscopy of PKC- θ (green) and vimentin (red) in activated Treg initially treated with either anti-CD25 mAb nanoparticles (left) or no nanoparticles (right) for 15 minutes. Arrows show enhanced PKC- θ localization on the vimentin basket. Data show one experiment representative of 3 **(b)** or 2 **(a)** independent experiments. **(c-d)** Flow cytometry analysis of vimentin expression in **(c)** freshly isolated Treg and CD4⁺ Tcon, or **(d)** Treg transfected with either control or vimentin siRNA. Graphs in **(c-d)** show composite data from 2 independent experiments, with n = 9/replicates per group. Data are representative of >10 independent experiments. *p<0.05; **p<0.01; ***p<0.001; ****p<0.0001 by unpaired *t*-test. MFI, median fluorescent intensity. Error bars=SEM.

Wild-Type

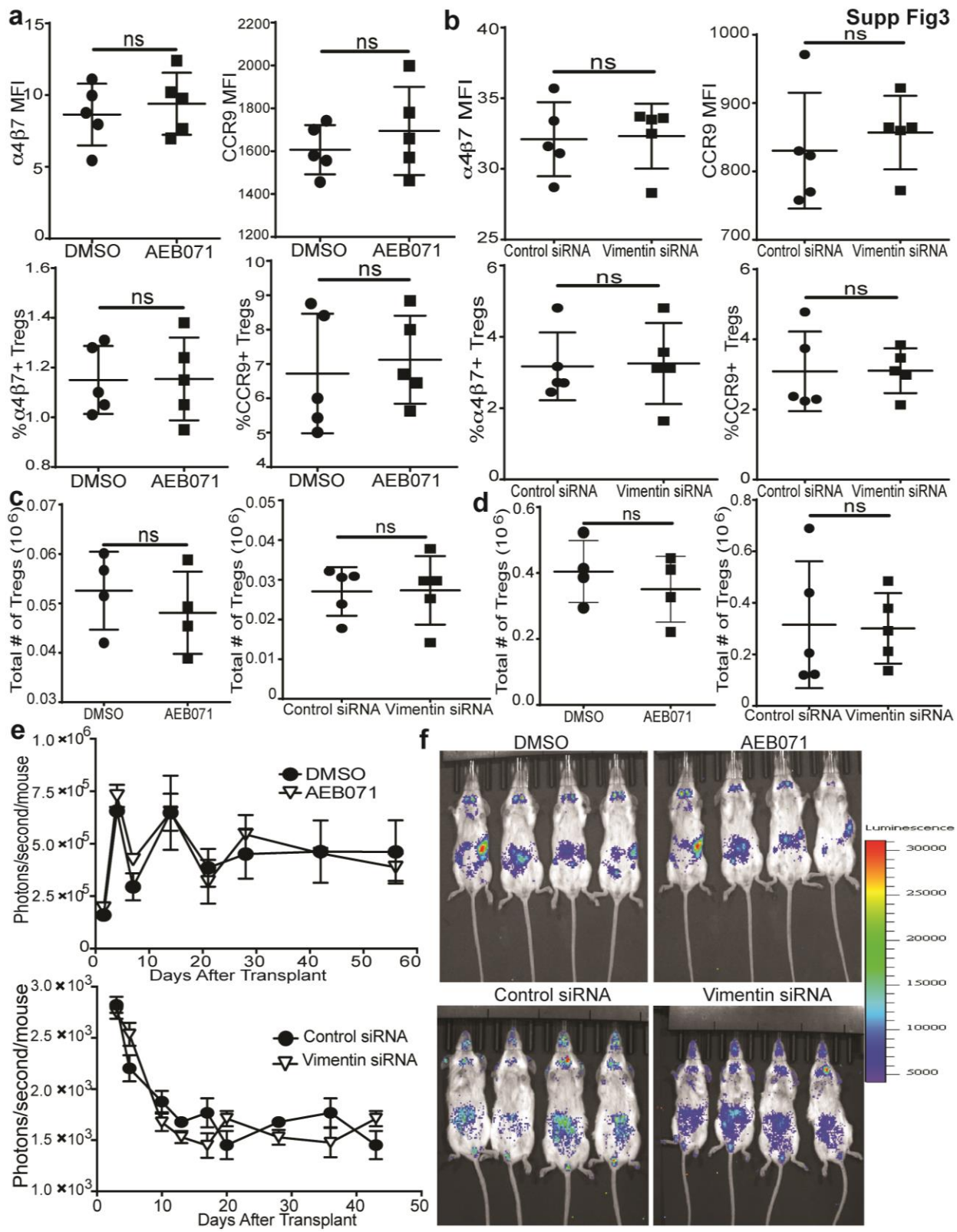
Side View

Vimentin siRNA

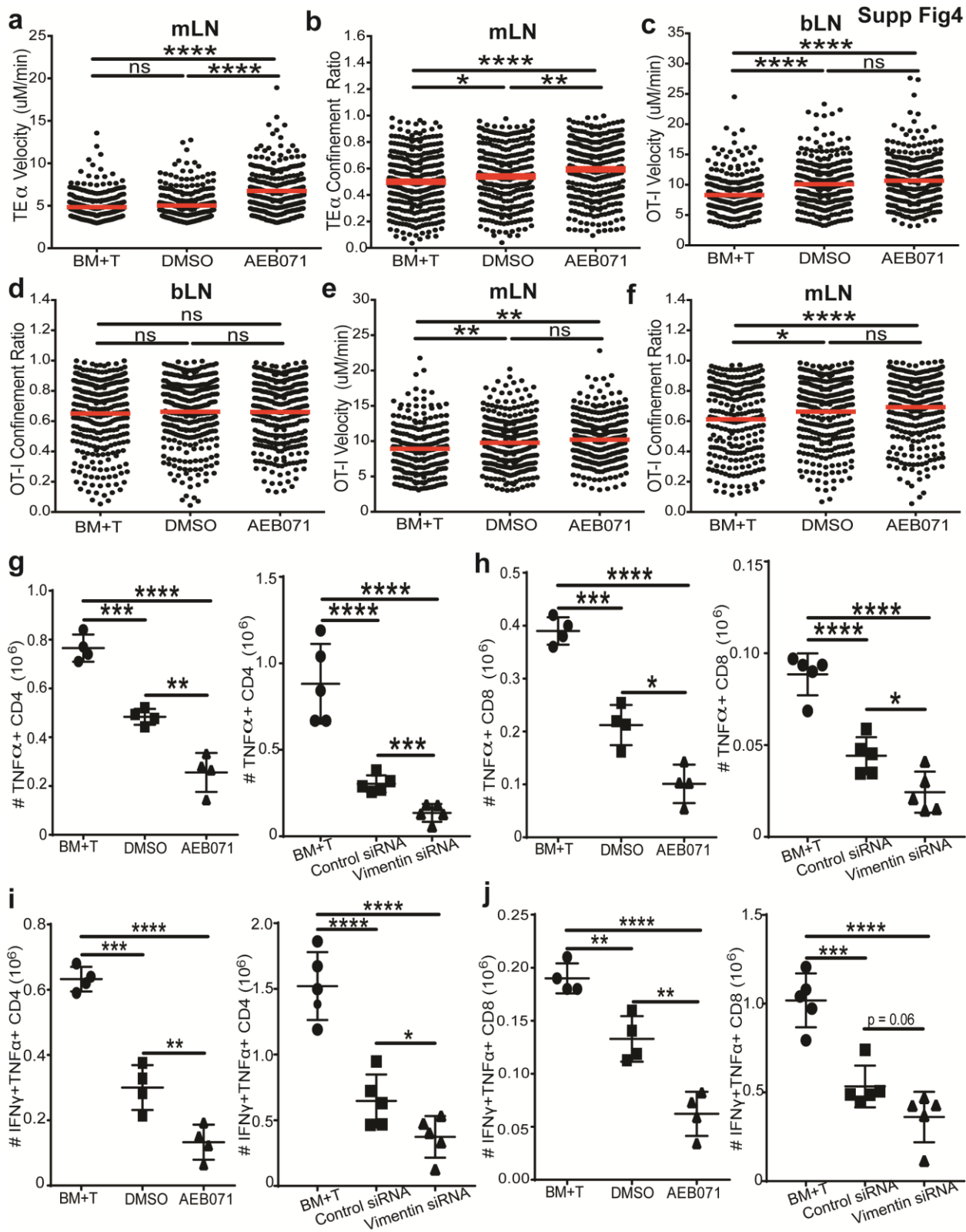


Supplementary Figure 2. Vimentin disruption augments Treg function *in vitro* and *in vivo*.

(a) Confocal microscopy of vimentin staining in activated wild-type and PKC- θ -KO Treg transfected with control or vimentin siRNA. (b-c) Percent suppression of (b) CD4⁺ Tcon proliferation by DMSO or AEB071 pre-treated wild-type Treg, (c) CD4⁺ Tcon proliferation by wild-type Treg transfected with control or vimentin siRNA, then treated with either DMSO or AEB07, and (d) CD4⁺ Tcon proliferation by wild-type Treg pre-treated with DMSO, AEB071, or C20 in a classical *in vitro* suppression assays. 1:1–1:9 indicates Treg:Tcon ratio. (e) Analysis of recipient mice weights after receiving BM only, BM+Tcon (BM+T), or BM+Tcon+Treg; Treg pre-treated with DMSO or AEB071. Data are pooled from 4 independent experiments; BM, n=25; BM+T, n=29; DMSO, n=29; AEB071, n=31. (f) Recipient mice weights, after receiving BM only, BM+T, or BM+Tcon+Treg; Treg transfected with control or vimentin siRNA. Data are pooled from 2 independent experiments; BM, n=10; BM+T, n=12; control siRNA, n=12; vimentin siRNA, n=12. Statistical comparisons in (d-e) are DMSO vs AEB071, and control vs vimentin siRNA, respectively. *p<0.05; **p<0.01; ***p<0.001; ****p<0.0001 by unpaired *t*-test, or one-way ANOVA with multiple comparison analysis and Tukey post-test. Error bars=SEM.

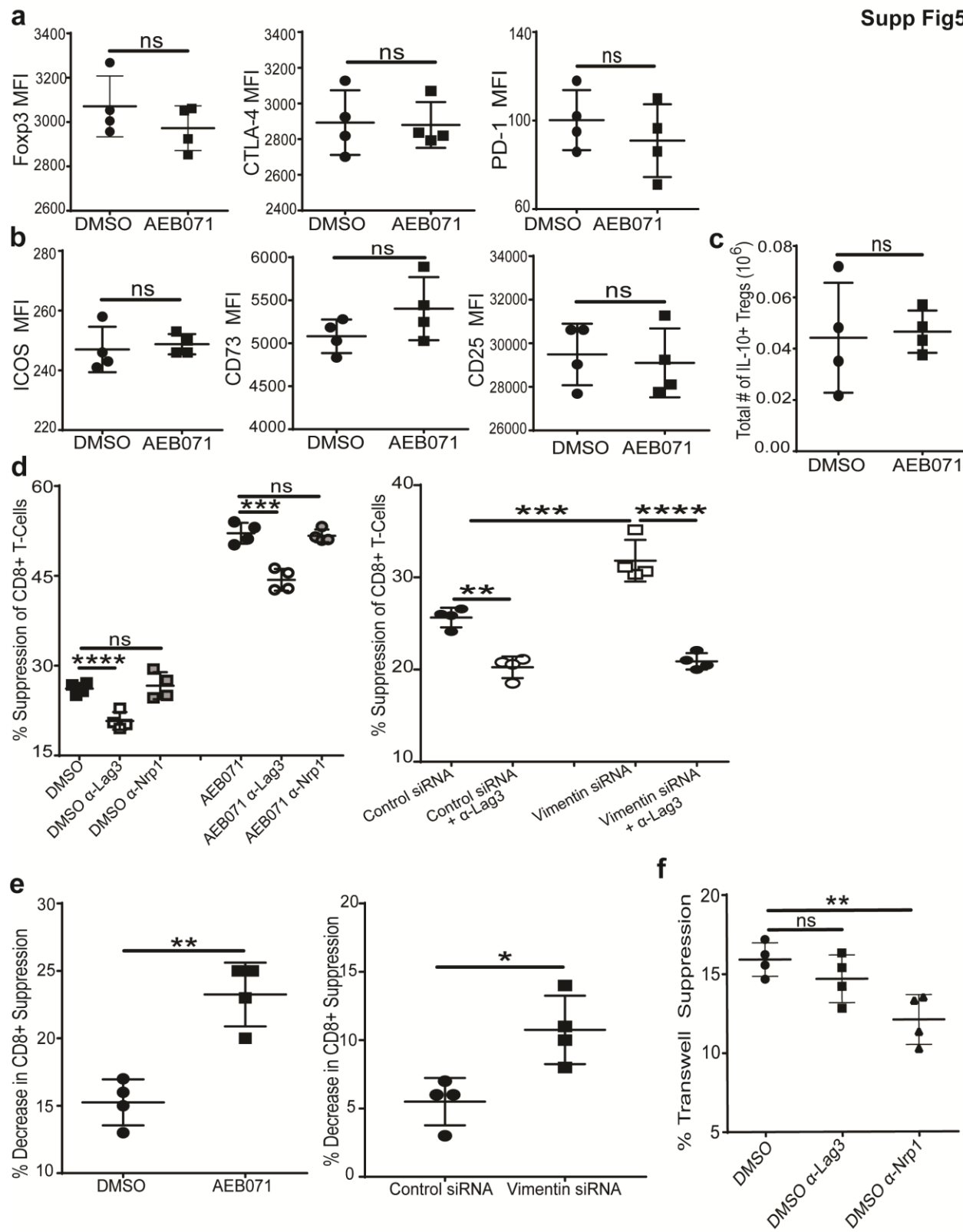


Supplemental Figure 3. Vimentin disruption does not alter Treg numbers or longevity *in vivo*. (a-b) GI homing molecule $\alpha 4\beta 7$ and CCR9 expression after activation of (a) DMSO or AEB071 treated, or (b) control or vimentin siRNA transduced, Treg. (c-f) Recipient mice were given BM+Tcon+Treg. Treg pre-treated with DMSO or AEB071; or transfected with control or vimentin siRNA. (c) Total number of small intestine LP Treg isolated from recipient LP on D14 after transplant, and (d) total number of splenic donor Treg on D7 after transplant. (e-f) Analysis of Treg persistence *in vivo* using luciferase-transgenic Treg and bioluminescent imaging of recipient mice. (e) There were no statistical differences in luminescence between mice given DMSO or AEB071 pre-treated Treg at any time-point (D1, 4, 7, 14, 21, 28, 42 and 56 shown), or between control siRNA and vimentin siRNA transfected Treg at any time point (D3, 5, 10, 13, 17, 20, 28, 36 and 43 shown). (f) Representative images of bioluminescence of recipients on D7 (DMSO/AEB071), or D5 (control/vimentin siRNA) after transplant. Data show one experiment representative of 3 (c-f) or 2 (a-b) independent experiments. n = 5 replicates/group for (a-b), n=4 or 5 mice/group for (c-f). *p<0.05; **p<0.01; ***p<0.001; ****p<0.0001 by unpaired *t*-test. MFI, median fluorescent intensity. Error bars=SEM.



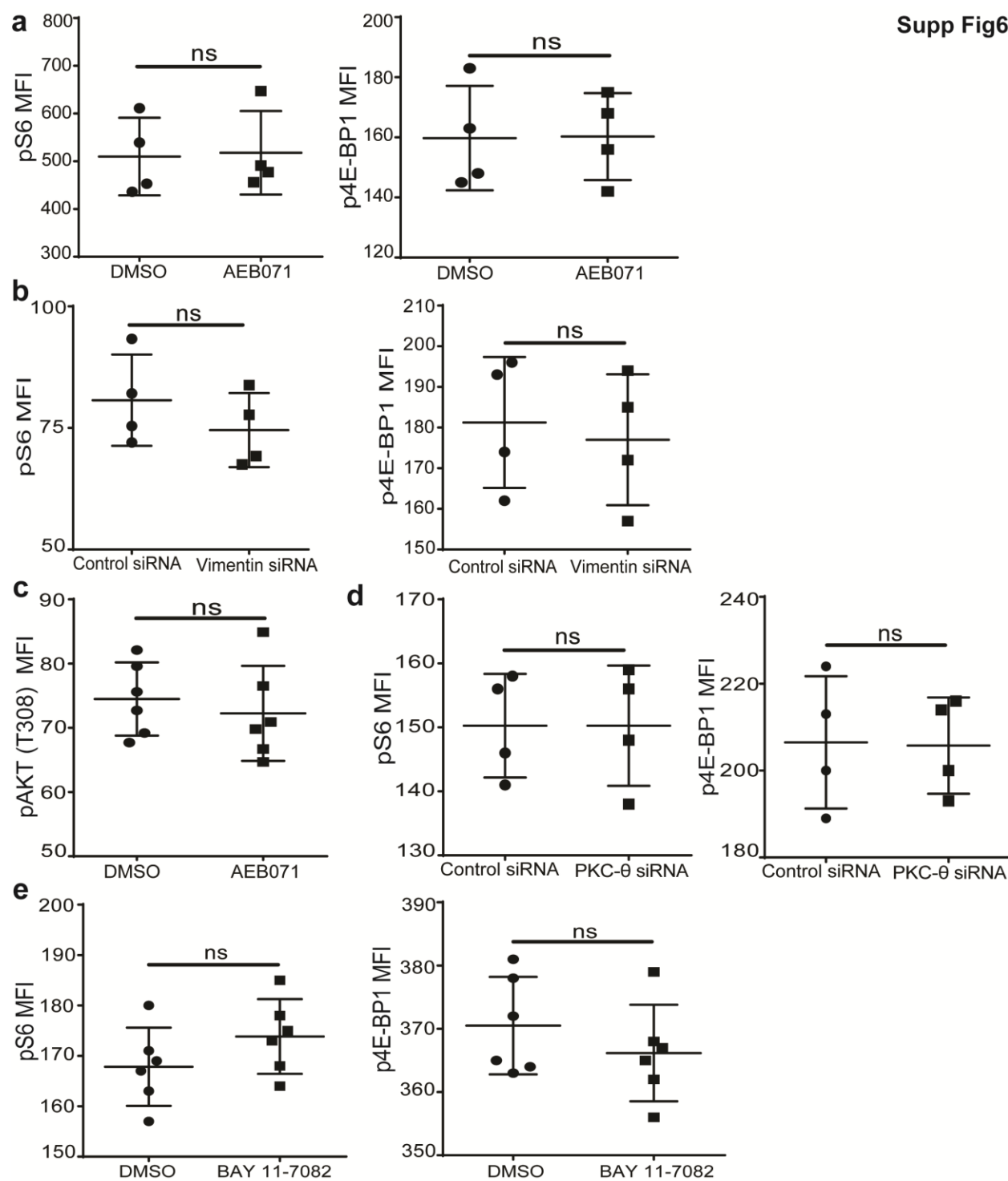
Supplementary Figure 4. Vimentin disruption increases Treg-mediated suppression of Tcon priming and function. (a-f) Multi-photon analysis of brachial (b-) and mesenteric lymph nodes (mLN) D4 after transplant from mice given BM, eGFP-TE α CD4 $^{+}$ and CMTMR-labeled OT-I CD8 $^{+}$ T-cells alone (BM+T), or Tcon with polyclonal Treg pre-treated with DMSO or AEB071. (a-b) Mean velocities and confinement ratios for each TE α cell in mLN. Mean velocities, confinement ratios for each OT-I cell in (c-d) bLN or (e-f) mLN. Dots represent single cells (n=300 cells/group) pooled from n=3 mice/group. Red line=data-set mean. (g-j) GVHD transplant with recipient mice given BM only, BM+Tcon (BM+T), or BM+Tcon+Treg. Treg pre-treated with DMSO or AEB071; or transfected with control or vimentin siRNA. Total number of IFN- γ^{+} (g) CD4 $^{+}$ and (h) CD8 $^{+}$ Tcon, and IFN- γ^{+} TNF- α^{+} (i) CD4 $^{+}$ and (j) CD8 $^{+}$ Tcon isolated from recipient small intestine LP on D14 after transplant. Data show one experiment representative of 3 individual experiments. 4 or 5 mice/group for (g-j), 3 mice/group for (a-f). *p<0.05; **p<0.01; ***p<0.001; ****p<0.0001 by unpaired *t*-test, or one-way ANOVA with multiple comparison analysis and Tukey post-test. Error bars=SEM.

Supp Fig5



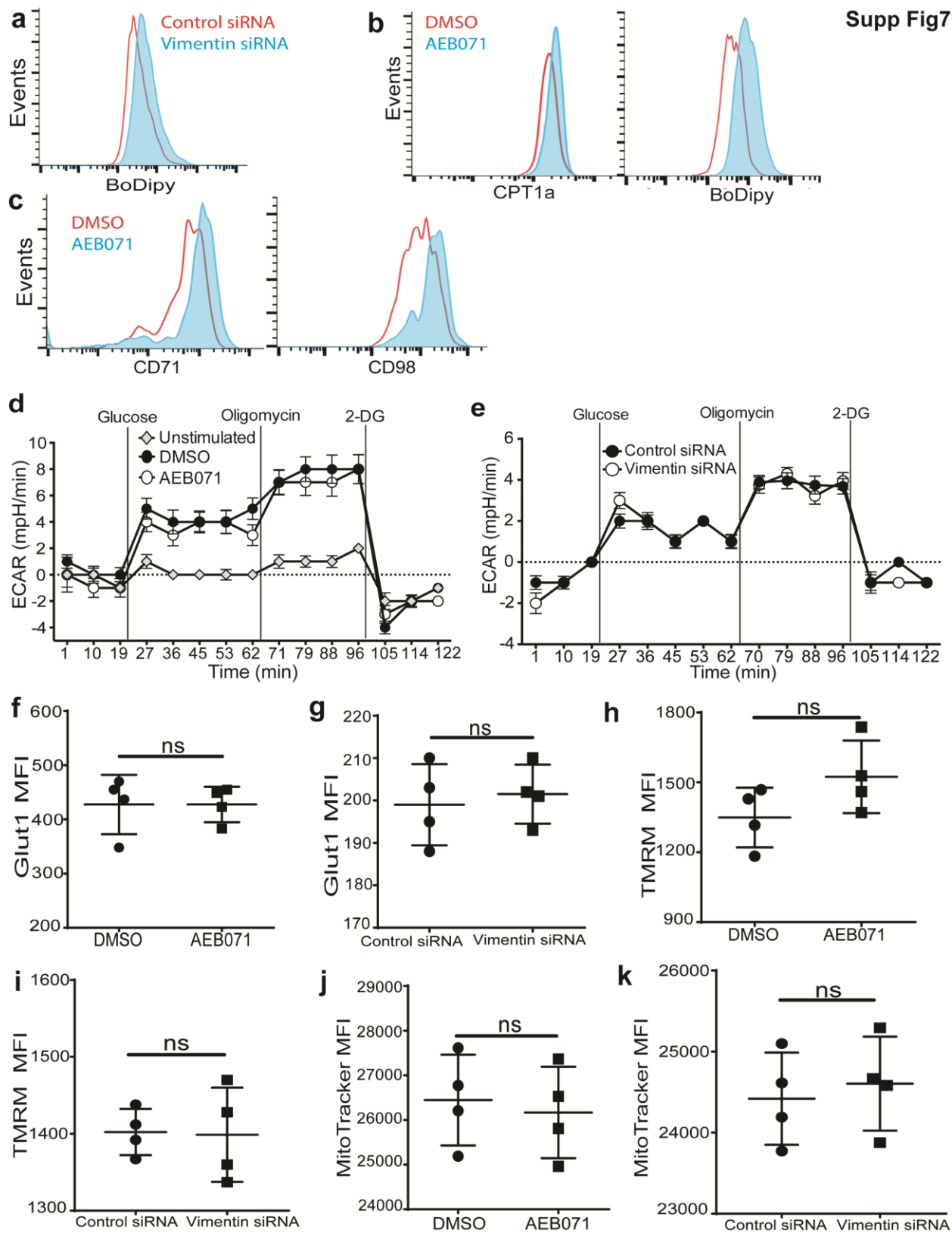
Supplementary Figure 5. Vimentin disruption increases Nrpl and Lag3 expression. (a-b) Analysis of Foxp3, CTLA-4, PD-1, ICOS, CD73 and CD25 MFI on DMSO and AEB071 pre-treated Treg after activation. (c) Analysis of the total number of IL-10⁺ Treg purified from the small intestine LP on D7 after transplant with BM+Tcon+Treg; Treg pre-treated with DMSO or AEB071. (d) Percent *in vitro* suppression of CD8⁺ Tcon proliferation by (left) DMSO/AEB071 pre-treated Treg or (right) control/vimentin siRNA pre-treated Treg cultured with either isotype, anti-Lag3, or anti-Nrpl blocking antibodies. Graph shows 1:3 Treg:Tcon ratio. (e) Quantification of the percent reduction in suppression of CD8⁺ Tcon with anti-Lag3 treatment in classical suppression assays shown in (d). (f) Percent *in vitro* transwell suppression of CD4⁺ Tcon proliferation by DMSO pre-treated Treg given either isotype, anti-Lag3 or anti-Nrpl blocking antibodies. Data show one experiment representative of 3 independent experiments. n=4 replicates/experiment for (a-b, d-f) and n=4 mice/group for (c). *p<0.05; **p<0.01; ***p<0.001; ****p<0.0001 by students *t*-test, or one-way ANOVA with multiple comparison analysis and Tukey post-test. MFI, median fluorescent intensity. Error bars=SEM.

Supp Fig6



Supplementary Figure 6. Vimentin disruption reduces mTORC2 activity. Analysis of S6 and 4E-BP1 phosphorylation in activated Treg **(a)** pre-treated with DMSO or AEB071, or **(b)** transfected with control or vimentin siRNA. **(c)** Analysis of Akt phosphorylation at Thr308 after stimulation of DMSO or AEB071 pre-treated Treg. **(d)** Analysis of S6 and 4E-BP1 phosphorylation in control or PKC- θ siRNA transfected Treg. **(e)** Analysis of S6 and 4E-BP1 phosphorylation in stimulated Treg pre-treated with DMSO or the IKK inhibitor BAY 11-7082. Data show one experiment representative of 3 **(a-c)** or 2 **(d-e)** independent experiments. n=6 replicates/group for **(e)** and n=4 replicates/group for **(a-d)**. *p<0.05; **p<0.01; ***p<0.001; ****p<0.0001 by students *t*-test. MFI, median fluorescent intensity. Error bars=SEM.

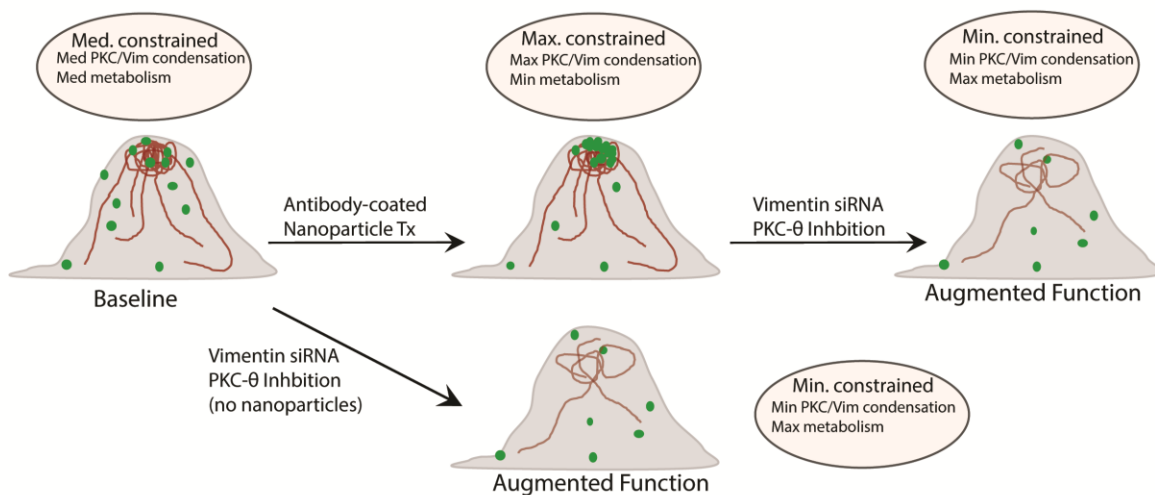
Supp Fig7



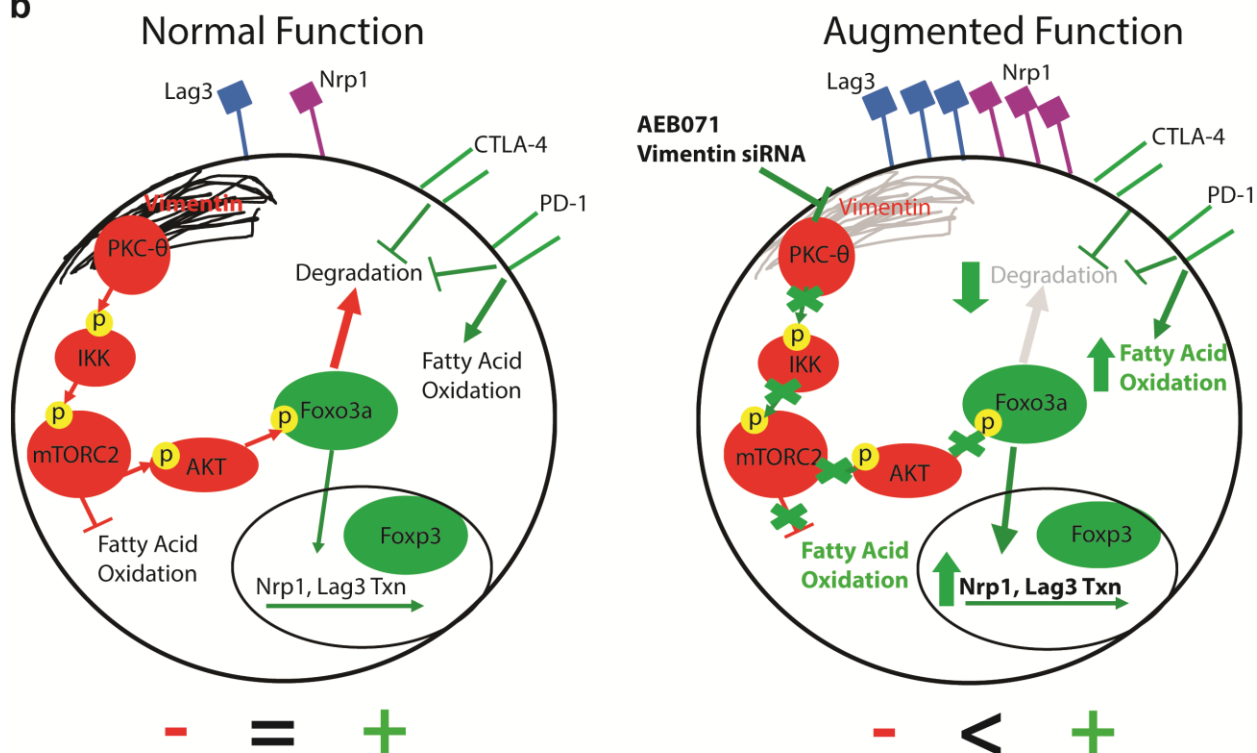
Supplementary Figure 7. Vimentin disruption increases Treg metabolic activity. (a-c)

Analysis of **(a-b)** BoDipy_{C1-C12} uptake and expression of **(b-c)** CPT1a, iron (CD71) and amino acid (CD98) uptake molecules, on splenic donor Treg **(a)** transfected with control or vimentin siRNA prior to transplant, or **(b-c)** pre-treated with DMSO or AEB071. Treg examination performed on D4 after transplant. Mice given BM+Tcon+Treg. **(d-e)** Analysis of extracellular acidification rate (ECAR) in stimulated Treg **(d)** pre-treated with DMSO or AEB071, or **(e)** transfected with control or vimentin siRNA. **(f-g)** Expression of Glut1 on splenic donor Treg on D4 after transplant with BM+Tcon+Treg. Treg pre-treated with **(f)** DMSO or AEB071, or **(g)** transfected with control or vimentin siRNA. **(h-k)** Analysis of **(h-i)** Tetramethylrhodamine, Methyl Ester, Perchlorate (TMRM) and **(j-k)** MitoTracker Deep Red staining in splenic donor Treg on D4 after transplant with BM+Tcon+Treg. Treg pre-treated with **(h,j)** DMSO or AEB071, or **(i, k)** control or vimentin siRNA. Data show one experiment representative of 3 independent experiments. n=4 mice/group for **(a-c, f-k)** and n=5 replicates/experiment for **(d-e)**. *p<0.05; **p<0.01; ***p<0.001; ****p<0.0001, by students *t*-test. MFI, median fluorescent intensity. Error bars=SEM.

a



b



Supplementary Figure 8. The effects of vimentin disruption on intracellular processes in Treg.

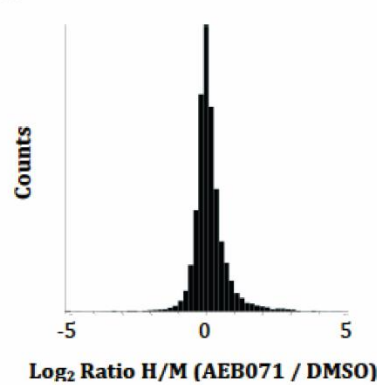
(a) Model demonstrating the effects vimentin siRNA and PKC- θ inhibitor treatment on antibody-coated nanoparticle treated or untreated Treg. On the left, a Treg at baseline is shown, with a “medium” level of constraint on function by PKC- θ /vimentin, with baseline levels of PKC- θ /vimentin condensation and metabolism. With antibody-nanoparticle treatment, PKC- θ /vimentin condensation is maximized, while metabolism is diminished. With vimentin siRNA or PKC- θ inhibitor treatment, regardless of antibody-nanoparticle treatment, constraint on Treg activity is minimized, as is PKC- θ /vimentin condensation, while Treg metabolism is maximized.

(b) Model demonstrating the effects of vimentin siRNA and PKC- θ inhibitor treatment on intracellular signaling in activated Treg. Highlighted in **red** are pathways that negatively regulate Treg function, including the downstream signaling associated with PKC- θ and vimentin. This pathway begins with vimentin and PKC- θ interacting at the DPC, and this results in a series of phosphorylation events that ultimately leads to inhibition of fatty acid oxidation and increased Foxo3a phosphorylation-mediated degradation. Highlighted in **green** are pathways that positively regulate Treg function, including signaling associated with Foxo3a nuclear localization (Nrp1, and Lag3 expression), as well as CTLA-4 and PD-1 signaling, which promote Foxo3a signaling and augment fatty acid oxidation, respectively. On the **left (normal function)**, an activated Treg without vimentin siRNA or AEB071 treatment. This Treg has a balance of positive (**green**) and negative (**red**) signaling, as denoted by the “- = +” shown below the cell. The net result of this balance between pathways is a Treg with “normal” or baseline function. On the **right (augmented function)**, an activated Treg previously treated with vimentin siRNA or AEB071. This Treg has reduced negative (**red**) regulatory signaling, as denoted by “x” marks over the signaling pathways downstream of PKC- θ /vimentin. The net result is signaling imbalance skewed towards positive input, as denoted by the “- < +” shown below the cell. The imbalance in signaling towards positive (**green**) inputs augments fatty acid oxidation and Foxo3a nuclear localization, which ultimately leads to increased Nrp1/Lag3 surface expression, and augmented Treg function. Yellow circle with “p” indicates phosphorylation. Abbreviations: Txn, transcription. PKC- θ , protein kinase C- θ ; IKK, I κ B kinase; mTORC2, mechanistic target of rapamycin complex 2; Nrp1, neuropilin-1; Lag3, lymphocyte-activation gene 3; CTLA-4, Cytotoxic T-lymphocyte associated protein 4; PD-1, programmed cell death protein-1.

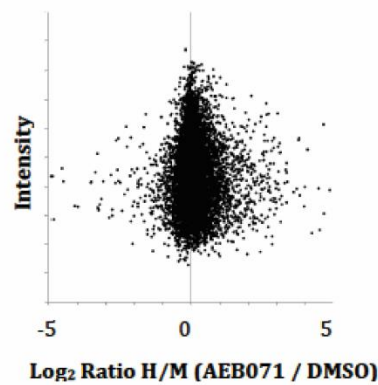
a

					Supp Table1				
Gene names	Average Log2 Ratio (H/M)	STD	pST	Sequence window	Gene names	Average Log2 Ratio (H/M)	STD	pST	Sequence window
ABI1	-2.4	0.25	232	SPGRTASLNQRPR	LRCH4	-2.8	0.26	432	GAPRKDSLKPKGL
ABI1	-3.3	0.46	223	SPARLGSGHSPGR	MAP3K2	3.4	0.64	514	LQTICLSGTGMKS
ABI3	-2.4	0.13	170	GTLRSRKSIPAT	MAP3K3	2.6	0.13	386	RNVPTKSPSAPIN
AHNAK	-2.3	0.42	4903	AKLSGSPSLKMPSL	MAP4K4	-2.4	0.26	550	QERSKPSFHAPEP
ANXA2	-2.5	0.27	44	PPSAYGSVKAYTN	MLLT4	-2.5	0.20	215	SFTRTISNPEVVM
ARAP2	-3.0	0.62	281	VSRPSRSFLLRHR	MYO1E	-2.0	0.25	980	YPHAPGSQRSNQK
ATAD5	-1.7	0.22	566	KLSRKTSIPVKDI	NOB1	-2.1	0.03	325	PRGLRYSLPTPKG
BAZ1B	-2.0	0.53	347	HLKKSLSGSPKLV	PTPN1	-2.5	0.55	378	SRVVGGSRLGAQA
CD4	-1.8	0.05	440	QIKRLLSEKKTQC	PTPN11	-2.3	0.43	595	LMQQQKSFRR
CD4	-2.2	0.73	433	RQAERMSQIKRLL	RBM39	-2.5	0.64	117	KIGLPHSILSR
CHD4	-1.7	0.04	303	KLGGFGSKRRSS	RLTPR	-2.1	0.46	1226	IGVSRGSGGAEGK
CIAPIN1	-2.4	0.26	177	SRQLKLSITKKSS	RPP38	-2.4	0.10	12	QAPGRGSLRKTRP
CNNM3	-2.2	0.02	467	VKRKPASLMAPLK	RUFY1	-3.4	0.17	165	GLKVKKFIGQNK
DBNL	-1.8	0.14	291	FLQKQLTQPETHF	SAMSN1	-2.3	0.19	142	KKMRAISWTMKKK
DDX3X	-3.6	0.23	90	FFSDRGSGSRGRF	SCAF4	-1.9	0.03	1004	ERFGRRSFGNRVE
DDX5	-2.3	0.26	30	SRAGPLSGKKFGN	SEC22B	-2.5	0.35	177	NNLSLSKKYRQD
DENND1C	-2.0	0.11	480	VLQRGGSLRAPAL	SHC1	-1.5	0.09	139	EWTRHGSFVNKPT
DENND4C	-2.5	0.31	948	LRNKRSSLYGIAK	SHKBP1	-1.7	0.09	662	RRRGGSFVERCQ
EDF1	-3.3	0.49	53	GQNKQHSITKNTA	SLK	-2.9	0.35	14	KIFKLGSEKKKKQ
EHBP1L1	-1.9	0.16	1273	PPRAHGFSHVRD	SMG5	-2.3	0.13	457	RKFSRLSLRRRR
EIF4B	-2.8	0.06	283	GRRAFGSGYRRDD	SP100	-1.9	0.06	59	LSTFRESFKRVI
EIF4H	-2.6	0.15	21	FGGGRGSRGSAGG	SPN	-3.7	0.40	291	TGALVLSRGGKRN
ENSA	-1.7	0.16	43	LKAKYPSLGQKPG	SPNS1	-2.4	0.34	563	VPQRGRSTRVPVA
EPB41	-1.8	0.66	709	EWDKRLSTHSPFR	STK10	-2.6	0.23	13	RRILRLSTFEKRK
FAM63A	-1.6	0.21	489	MRTRVLSLQGRGA	STX5	-2.6	0.09	9	PRKRYGSKNTDQG
GMIP	-1.7	0.03	907	TSVPRGSLRGRGP	TBC1D9B	-1.7	0.11	275	RPHRNISALKRDL
HIST1H1E	-3.0	0.31	104	GTGASGSKLNKK	TPD52L2	-2.1	0.52	161	LGDMRNSATFKSF
HMGB1	-2.2	0.52	53	ERWKTMSAKEKGK	TUBGCP3	-2.9	0.31	896	EPRLRVSLGTRGR
IFI16	-4.6	0.49	95	VKGPALSRRKKKE	UBE2M	-2.8	0.21	6	_MIKLFSLKQQKK
IL16	-3.0	0.12	795	PAWFRQSLKGLRN	UFD1L	-3.4	0.06	335	FSGEGQSLRKKGR
INPP5D	-1.9	0.05	1085	PAPRLRSFTCSSS	UVRAG	-2.1	0.04	689	LNENVSSFRRPRR
IRF2	-3.4	0.15	119	PLSERPSKKGKKP	VIM	-1.38	0.07	25	GTASRPSSRSYV
KCNAB2	-2.2	0.19	14	GSPARLSLRQTGS	WIPF1	-1.9	0.23	276	PVGNRPSIHREAV
LNPEP	-1.4	0.00	91	SSGLRNSATGYRQ	WIPF1	-1.8	0.04	234	TALGGGSIRQSPL

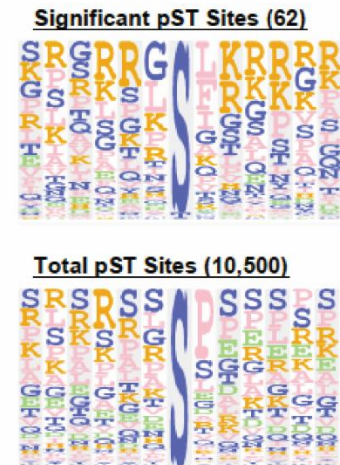
b



c



d



Supplementary Table 1. AEB071 treatment results in reduced phosphorylation of 68 phosphorylation sites. (a) Results of liquid chromatography–mass spectrometry (LC-MS) analysis of phosphorylation changes at conserved PKC- θ serine and threonine phosphorylation sites in DMSO and AEB071 treated, SILAC labeled human Treg. Column 1 shows the gene names for the phosphorylated proteins. Column 2 shows alterations in phosphorylation indicated by the average log₂ ratio of ion intensity for each phosphopeptide (AEB071/DMSO). Negative values indicate reduced phosphorylation in AEB071 treated samples compared to DMSO. A total of 68 phosphorylation sites on 66 proteins had reduced phosphorylation after AEB071 treatment. Sequence window (column 5) shows 12-14 amino acids around the altered serine or threonine phosphorylation site. Phosphosite (pST) indicates the position in the protein sequence of the amino acid on which the phosphorylation change occurred. STD, standard deviation. (b) Plot of frequency (y-axis) vs. log₂ ratio of abundance of phosphopeptides from AEB071 stimulated Tregs over-abundance of phosphopeptides from unstimulated Tregs (x-axis). (c) Scatter plot of mass spectral signal intensity (y-axis) vs. log₂ ratio of abundance of phosphopeptides from AEB071 stimulated Tregs over-abundance of phosphopeptides from unstimulated Tregs (x-axis). (d) Frequency of the most common amino acids surrounding significantly changed phosphorylation sites (top) and all phosphorylation sites detected in this study (bottom). Graphs show the relative frequencies for each amino acid (as noted by sized), and not a specific sequence of amino acids.